

# Oxidation of Stainless Steel in the High Velocity Oxy-Fuel Process

K. Dobler, H. Kreye, and R. Schwetzke

(Submitted 2 February 2000)

The high velocity oxy-fuel (HVOF) spray process has been primarily used for the application of wear-resistant coatings and, with the introduction of new, more powerful systems, is being increasingly considered for producing corrosion-resistant coatings. In this study, the influence of various spray parameters for the JP-5000 and Diamond Jet (DJ) Hybrid systems on the oxidation of stainless steel 316L is characterized. Experimental results reveal that coating oxygen contents of less than 1 wt.% can be more easily attained with the JP-5000 than the DJ Hybrid systems because of the former's design. In both cases, however, the low particle temperatures necessary for low oxygen content coatings may impair bond and cohesive strength. Heat treating the coatings after processing reduces hardness, metallurgically enhances bond strength, and enables the spheroidization of oxide layers surrounding unmelted particles.

An empirical model describing oxidation in the thermal spray process was expanded to explain the oxidation in the HVOF spraying of stainless steel. It was concluded that for these oxygen-sensitive materials, maintaining a relatively low particle temperature throughout the spray process minimizes oxygen pickup by preventing an autocatalytic oxidation process and particle fragmentation upon impact. For the DJ Hybrid systems, understoichiometric fuel settings are selected, whereas for the JP-5000, oxygen-rich mixtures are preferred.

**Keywords** 316L, corrosion, HVOF, oxidation, stainless steel

## 1. Introduction

High velocity oxy-fuel (HVOF) flame spraying has been recognized as the most significant development in the thermal spray industry during the last 15 years. Since the initial use of tungsten carbide-cobalt, the range of powders has expanded to include a large variety of other carbides as well as metallic and ceramic materials. The HVOF coatings have proven themselves superior in wear-resistant applications.<sup>[1]</sup> In addition to the introduction of new spray systems, capable of generating particle velocities 30 to 50% higher than their predecessors,<sup>[1]</sup> this process is being increasingly recognized as a means of producing denser and more corrosion-resistant coatings.

For industrial applications requiring a high degree of corrosion resistance, austenitic stainless steels or nickel-base alloys are generally employed in either bulk form or applied as overlays or coatings. Applying these metals by atmospheric thermal spraying, however, leads to the formation of oxides, which in turn impair corrosion resistance and mechanical properties.<sup>[2]</sup> The ability to control coating oxygen content is therefore essential for attaining the maximum corrosion resistance.

This study focuses on characterizing the oxidation of HVOF sprayed austenitic stainless steel 316L using the JP-5000 and Diamond Jet (DJ) 2700/2600 systems. By assessing the influence of various spray parameters on oxygen content and the microstructure of the coatings and then correlating them to the mechanical properties, parameters may be tailored to produce optimum coatings. Moreover, the knowledge gained from this material system can be extended to numerous others.

**K. Dobler, H. Kreye, and R. Schwetzke**, Universitat der Bundeswehr Hamburg, 22042 Hamburg, Germany. K. Dobler is presently with St. Louis Metallizing Co., Saint Louis, MO, USA. R. Schwetzke is presently with Inometa GmbH, 32052 Herford, Germany.

## 2. Coating Oxidation

The formation of oxides during the thermal spray process can be categorized into three time or spatial regions, as shown in Fig. 1. Some of the conditions influencing oxidation during HVOF processing, as described by Hackett and Settles,<sup>[3,4]</sup> are given in Table 1. Region I starts at the point of particle injection within the nozzle and extends to the end of the jet core. In this zone, particles are exposed to flame's high temperatures as well as its combustion products. While the amount of free oxygen can be controlled *via* the oxygen/fuel (O/F) ratio, it must be remembered that even at understoichiometric settings, the flame still contains different oxidizing combustion products, and thus particle oxidation cannot be completely avoided. Region II refers to the time from when the entrained atmosphere reaches the centerline of the flame until the particles impact upon the substrate. In this zone, the atmosphere will contain up to 20% oxygen. Finally, region III encompasses the time the particles spend on the substrate after impact until the next layer covers them. During this period, the individual splats are still exposed to the oxidizing effects of the flame and may undergo considerable oxidation. Although the temperatures are low as compared to those within the flame, the exposure time to the atmosphere is at least several times greater.

The contribution of the different oxidation mechanisms to the oxygen content of a coating depends not only upon the spray parameters, but also on the spray powder feedstock. According to Zimmermann and Kreye,<sup>[5,6]</sup> the oxidation of HVOF sprayed pure molybdenum is dominated by conditions created in region I. By merely varying the type of fuel gas and the O/F ratio, the oxygen content of the coating can be predetermined for values between 3 and 11% (all oxygen contents in weight percent). The amount of oxygen absorbed by molybdenum in regions II and III is almost constant and varies only slightly with the particle temperature. On the other hand, oxidation during plasma spraying of molybdenum can obviously only occur in regions II and III,

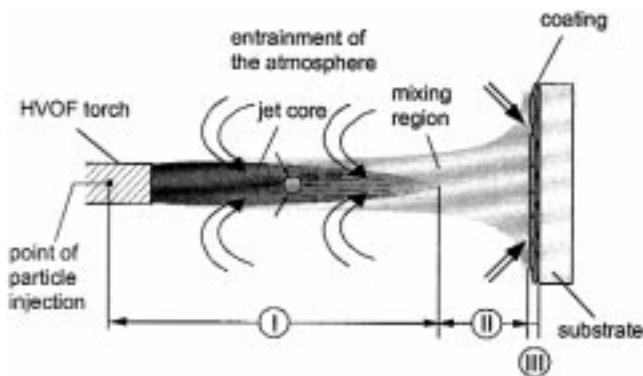


Fig. 1 Schematic of the oxidation in the HVOF process

Table 1 Description of the oxidation process in HVOF flame spraying<sup>[3]</sup>

	Region I	Region II	Region III
Estimated fraction O <sub>2</sub>	~2%	~20%	~20%
Exposure time	~0.001 s	~0.001 s	0.01–0.02 s
Relative temperature	High	Medium	High, then low
Particle shape	Sphere	Sphere	Splat

and the range of oxygen pickup lies between 1.8 and 4.2%. Recent work by Kreye<sup>[7]</sup> has revealed that the oxidation of copper essentially takes place in region III. When powder was sprayed into water at a distance of 800 mm, the oxygen content remained constant at 0.2%. After spraying the same feedstock onto a substrate at a stand-off distance of 250 mm, the oxygen content rose to 0.5%. Similarly, Hackett and Settles<sup>[4]</sup> reported that about 75% of the oxidation of iron particles during spraying with the JP-5000 system occurs in regions II and III. Here, the use of an inert gas shroud curtailed coating oxygen content from 3.2 to 0.9%. However, this method may be impractical on an industrial scale, as about 1500 m<sup>3</sup>/h of nitrogen was necessary to attain these results. It should also be noted that the experiments were conducted with a single understoichiometric flame setting. Vardelle *et al.*<sup>[8]</sup> examined the rate-controlling phenomena for the oxidation of iron particles in the free plasma jet and on the splat surface. They concluded that oxidation occurs primarily during the time of exposure of the hot splats to the ambient atmosphere and to the process gas jet. Neiser *et al.*<sup>[9]</sup> examined the splat interface of HVOF wire sprayed mild steel coatings. Their results support the hypothesis that, for these conditions, inflight oxidation of the particles is the dominant mechanism.

Moskowitz and Lindley's<sup>[10]</sup> investigations with the Jet Kote system (Deloro Stellite, Goshen, IN) reveal that the O/F ratio is the most significant parameter for spraying low oxygen content coatings of SS 316L and Hastelloy C. A severely understoichiometric hydrogen/oxygen flame minimizes the presence of oxygen from region I. A further reduction in oxygen pickup is attained *via* an inert helical shroud that shields the particle stream without compromising particle temperature. Based on research conducted with the JP-5000 system, Voggenreiter *et al.*<sup>[11]</sup> concluded that the key to producing low oxygen content stainless steel coatings is to spray the particles cold enough so that no fragmentation occurs upon impact. Particles that are molten

upon impact fragment and tremendously increase the area exposed to the atmosphere. The nonintuitive solution for reducing oxidation was to use overstoichiometric settings.

The present investigations therefore focus on decreasing oxidation *via* the spray parameters as well as understanding and resolving the apparently contrasting effect of the O/F ratio on the coating oxygen content observed with the different HVOF spray systems.

### 3. Experimental

In this investigation, gas-atomized stainless steel 316L powders with size distributions of primarily  $-45 + 16 \mu\text{m}$  and some  $-53 + 22 \mu\text{m}$  were used as powder feedstock and deposited to thicknesses between 300 and 800  $\mu\text{m}$  on three different types of substrates:  $70 \times 50 \times 4 \text{ mm}$  mild steel sheets,  $250 \times 70 \times 0.5 \text{ mm}$  foils, and steel cylinders with a 25 mm OD. Spraying was conducted with three different HVOF systems: a Tafa JP-5000 (Tafa, Inc. Concord, NH) fueled by kerosene; and two Sulzer Metco (DJ) Hybrid systems, a DJ 2700 operated with propane or ethylene, and a DJ 2600 powered by hydrogen. Schematic diagrams of the systems are shown in Ref 1. Additionally, powder particles were sprayed into water at distances of 800 and 1000 mm for the DJ Hybrid and JP-5000 systems, respectively. Selected specimens were heat treated under three different conditions: (1) for 10 minutes at 1050 °C in an evacuated quartz tube ( $<1 \times 10^{-2} \text{ mbar}$ ), (2) for 2 h at 1100 °C at the same vacuum conditions as in (1), and (3) for 2 hours at 1100 °C in a high vacuum oven ( $<1 \times 10^{-5} \text{ mbar}$ ). The spray parameters were varied within the ranges shown in Table 2.

The microstructures of the powders and coatings were characterized by optical and scanning electron microscopy. Microhardness measurements were conducted on polished cross sections using a Vickers diamond pyramid indenter and a load of 300 g (HV 0.3). A minimum of ten readings was taken per specimen. The bond strength was determined in accordance with DIN EN 582 using cylindrical specimens with a diameter of 25 mm. Oxygen content measurements were performed with a Leco Oxygen/Nitrogen Analyzer, Model TR-436DR (Leco Corporation, St. Joseph, MI). Coatings were removed from the thin steel foils, pulverized, and degreased. A minimum of three readings was taken per specimen.

In order to evaluate the corrosion resistance of the coatings, the specimens underwent a test typically employed in the electroplating industry. In the Kesternich test, performed according to DIN 50018, the coated specimens were exposed to a saturated atmosphere of sulfur dioxide. Specimens were prepared by covering the entire sample, except for a  $40 \times 20 \text{ mm}$  area on the coating, with a corrosion-resistant lacquer and then placed into a 300 L leak proof chamber. The coatings were exposed to 25 cycles, whereby each cycle is composed of two stages. In the first stage, the chamber is filled with 2 L of distilled water and 2 L of sulfur dioxide, heated to  $40 \pm 3 \text{ }^{\circ}\text{C}$  within 90 minutes, and maintained at this temperature for 8 h. In the second stage, the chamber is ventilated for 16 h at room temperature. Before each cycle, all water was removed from the chamber and replenished with fresh water and sulfur dioxide. After 2 and 25 cycles, the samples were inspected visually according to DIN EN ISO 1462 and metallographically.

**Table 2 Range of spray parameters for the various systems**

HVOF system	Fuel	Fuel flow rate(a), l/h, m <sup>3</sup> /h	Oxygen flow rate, m <sup>3</sup> /h	Oxygen/fuel ratio(b,c)	Normalized O/F ratio, $\lambda$	Powder feed rate, g/min
JP-5000	Kerosene	16.3–26.1	43.9–69.4	2.8–5.5	0.8–1.6	110–225
DJ 2700	Propane	3.0–5.4	7.5–19.9	3.0–5.7	0.6–1.1	80–140
DJ 2700	Ethylene	5.0–6.8	8.0–22.8	1.8–4.5	0.6–1.5	80–85
DJ 2600	Hydrogen	38.8	9.9–12.9	0.36–0.45	0.7–0.9	75–80

(a) Unit of measurement for kerosene is l/h; for fuel gases, m<sup>3</sup>/h

(b) Includes the oxygen fraction of the compressed air for the DJ Hybrid systems

(c) Stoichiometric O/F ratio ( $\lambda = 1$ ) for propane is 5; for hydrogen, 0.5; for ethylene, 3; and for kerosene, 3.4**Table 3 Oxygen content of the SS 316L coatings**

HVOF System	Fuel	Oxygen content, wt.%		
		$\lambda < 0.9$	$0.9 \leq \lambda \leq 1$	$\lambda > 1$
JP-5000	Kerosene	3.6	1.8	0.4–0.8
DJ 2700	Propane	0.6–2.7	1.0–3.8	7.5
DJ 2700	Ethylene	1.3–1.6	2.1–6.9	...
DJ 2600	Hydrogen	0.9–1.2	7.2–7.4	...

## 4. Results and Discussion

### 4.1 Oxygen Content and Coating Microstructure

Table 3 enumerates the results of the oxygen content measurements according to the normalized O/F ratio,  $\lambda$ , range. The powder feedstock had an oxygen content of about 0.02%, and as can be readily elucidated, the extent of oxygen pickup varied with the spray system and parameters. Of most importance is the fact that the JP-5000 reduces oxygen content with overstoichiometric conditions, whereas the DJ Hybrid systems use understoichiometric parameters to attain low oxygen contents.

In Table 4, properties of coatings produced with the JP-5000 system are presented, whereby the reference parameters are  $\lambda = 1.35$ , combustion chamber pressure 0.66 MPa, and stand-off distance 360 mm. The most influential factor affecting oxygen content was the O/F ratio. At a constant chamber pressure of 0.66 MPa, the oxygen content of the coatings decreased from 3.6 to 0.38% as  $\lambda$  was increased from 0.82 to 1.62. To a lesser extent, chamber pressure also affected coating oxygen content. At  $\lambda = 1.35$ , the content is reduced from 0.64 to 0.51% as the chamber pressure is decreased from 0.72 to 0.59 MPa. Likewise at  $\lambda = 1.47$ , the oxygen content is lowered from 0.76 to 0.50% as pressure is decreased from 0.84 to 0.66 MPa. Lastly, the use of coarser powder ( $-53 + 22 \mu\text{m}$  instead of  $-45 + 16 \mu\text{m}$ ) reduced the content from 0.58 to 0.38% at reference conditions of  $\lambda = 1.35$  and a pressure of 0.66 MPa.

The properties of coatings sprayed with the DJ Hybrid system are presented in Tables 5 and 6. The reference parameters for coatings sprayed with propane are  $\lambda = 0.9$ , fuel gas flow rate,  $4.1 \text{ m}^3/\text{h}$ , and stand-off distance, 250 mm. The wide range of the resultant oxygen content is primarily determined by the type of gases used and the respective O/F ratios. When operating the DJ 2700 with propane, oxygen contents ranged from 0.6 to 7.5%, whereby at  $\lambda < 0.9$ , the contents remained between 0.6 to 2.7%. As  $\lambda$  was increased from 0.9 to 1.14, the oxygen contents jumped from 1.8 to 7.5%. Likewise, deposits sprayed with hydrogen also revealed high sensitivity to increasing flame temperature as the oxygen contents jumped from 1.2 to 7.4 % when  $\lambda$  was set closer to stoichiometry. Similarly, the contents of coat-

ings produced with ethylene increased from 1.6 to 6.9% as the flame was changed from fuel rich to stoichiometric conditions.

The gas flow rate played a salient role as well. For propane, oxygen contents were reduced from 2.1 to 1.0% at  $\lambda = 0.9$  when the gas flow rate was decreased by 30%. At  $\lambda = 0.7$ , oxygen concentration was reduced from 2.7 to 0.7% when the gas flow rate was decreased by 35%. When spraying with ethylene at stoichiometric conditions, oxygen contents lowered from 6.9 to 2.1% as the gas flow rates were reduced by 25%.

With regard to stand-off distance, no discernible trend could be detected for propane flames when the coatings had an oxygen content of between 2 and 3%. However, low oxygen content coatings produced with hydrogen and ethylene gases show reductions from 1.2 to 0.9% and 1.6 to 1.4%, respectively, as stand-off distance was lengthened from 250 to 350 mm. When spraying with propane at  $\lambda = 0.9$ , the lack of air cooling, reducing the translational velocity by 50% or augmenting the feed rate from 80 to 140 g/min, resulted in raising oxygen contents from 2.1 to 3.2 to 3.8%.

Various microstructures of the DJ Hybrid processed 316L coatings are shown in Fig. 2. The typical microstructure of a coating containing less than 1% oxygen is presented in Fig. 2(a), whereby a high percentage of half-moon-shaped, partially melted particles is characteristic for these coatings. To attain this microstructure, the powder temperature must remain low enough to permit only a small amount to melt. The micrograph in Fig. 2(b) presents the typical microstructure of coatings whose individual spray layers are apparent *via* oxide layers and clusters as well as being characterized by a decrease in the number of unmelted particles. These features are more obvious when spraying conditions are altered to augment flame and thus particle temperature. Oxide layers grow on each layer due to higher surface temperatures in comparison with less oxidized coatings. Lastly, Fig. 2(c) clearly reveals the individual oxide and metal layers as well as the numerous, porous oxide clusters, which roughen the coating surface. Here, the particles were heated high enough that a considerable percentage of each particle is molten upon impact. These particles will splash or fragment and the surface area exposed to the atmosphere will tremendously increase and accordingly enhance the degree of oxidation. In addition, the relatively large amount of heat present at the coating surface facilitates the growth of the oxide layer and clusters. The roughness due to these formations may, in turn, further foster particle fragmentation.

The microstructure shown in Fig. 3(a) represents coatings typically produced by the JP-5000 system. As can be readily observed, the microstructure is dominated by unmelted particles and accordingly has low oxygen contents. Figure 3(b) and (c)

**Table 4** Properties of coatings produced with the JP-5000

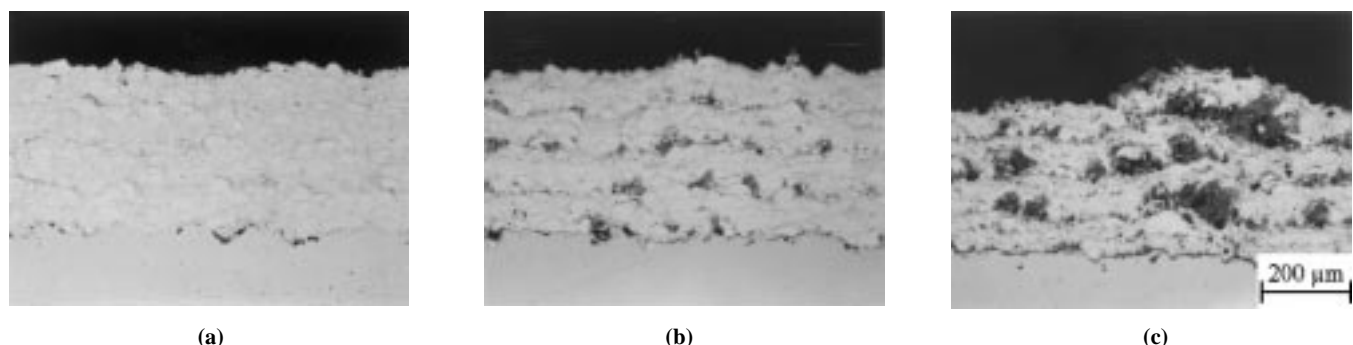
Chamber pressure, MPa (psi)	Fuel flow rate, l/h	Normalized oxygen/fuel ratio $\lambda$ , (O/F ratio)	Oxygen content, wt. %	Bond strength, MPa	Hardness, HV 0.3
0.59 (85)	17.0	1.35 (4.6)	0.51	33	302
	26.1	0.82 (2.8)	3.61	56	380
	23.1	1.00 (3.4)	1.73	49	354
0.66 (95)	18.9	1.35 (4.6)	0.58	48	320
	17.8	1.47 (5.0)	0.50	48	290
	16.3	1.62 (5.5)	0.38	39	290
0.72 (105)	20.8	1.35 (4.6)	0.64	43	323
0.84 (122)	22.7	1.47 (5.0)	0.76	56	370

**Table 5** Properties of coatings produced with the DJ Hybrid operating on propane

Fuel flow rate, m <sup>3</sup> /h	Normalized oxygen/fuel ratio $\lambda$ (O/F ratio)	Oxygen content, wt. %	Bond strength, MPa	Hardness, HV 0.3
3.0	0.90 (4.5)	0.97	43	254
	0.60 (3.0)	0.56	39	254
	0.70 (3.5)	0.69	52	290
4.1	0.80 (4.0)	0.81	50	306
	0.90 (4.5)	2.05	57	377
	1.14 (5.7)	7.50	48	455
5.4	0.70 (3.5)	2.70	52	415

**Table 6** Properties of coatings produced with the DJ Hybrid operating on hydrogen and ethylene

Fuel gas Fuel flow rate, m <sup>3</sup> /h	Normalized oxygen/fuel ratio $\lambda$ (O/F ratio)	Oxygen content, wt. %	Bond strength, MPa	Hardness, HV 0.3
<b>Hydrogen</b>				
38.8	0.72 (0.36)	1.16	57	333
	0.88 (0.44)	7.42	59	429
<b>Ethylene</b>				
5.0	1.00 (3.0)	2.05	52	357
6.8	0.62 (1.85)	1.56	58	344
	1.00 (3.0)	6.89	59	429

**Fig. 2** Microstructure of DJ Hybrid sprayed 316L stainless steel coatings with various oxide contents. (a) Low oxide content, 0.97 wt. % O. (b) Medium oxide content with oxides on the individual spray layers, 1.75 wt. % O. (c) High oxide content with oxide clusters, 3.58 wt. % O

present atypical oxidized structures for this spray system. The percentage of unmelted particles is lower and the amount of oxides larger, indicating that the particles were heated to a greater degree.

#### 4.2 Oxidation Model

According to the model schematically depicted in Fig. 1, the oxidation process can be categorized into three regions, each

being influenced by various spray parameters. In addition, the properties of the materials being sprayed must be carefully considered. Based on the oxygen content results and the microstructural evaluations, it has been concluded that the oxidation process of stainless steel can best be described from the perspective of particle temperature.

At relatively low particle temperatures, the rate of oxidation or the amount of oxygen pick-up in each region is low. This is due to the fact that the particles are barely melted by the flame

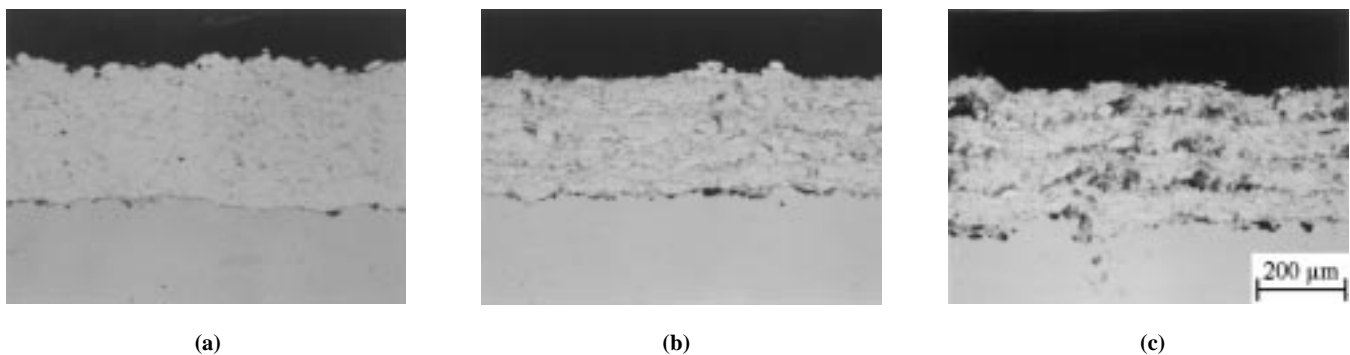


**Fig. 3** Microstructure of 316L stainless steel coatings sprayed with JP-5000. (a) Typical coating with low oxide content and plenty of unmelted particles, 0.50 wt.% O. (b) and (c) Higher oxide contents and decreasing amount of unmelted particles, 1.73 and 3.61 wt.% O

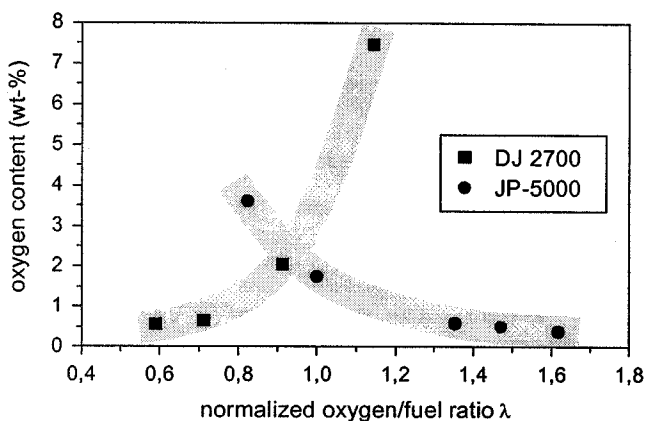


**Fig. 4** Effect of normalized oxygen/fuel ratio  $\lambda$  on the oxide content of the coatings

and are heavily dependent on the drag forces of the flame to achieve the high velocities necessary for a good adhesion to the substrate.

As temperature increases, the contribution of each region is larger, resulting in a greater oxygen content overall. Obviously, diffusion and thus oxidation rates are higher. In addition, an autocatalytic oxidation process must serve to drive these rates even higher *via* the heat that is released during the formation of oxides. The contribution of oxidation in region I may be the same as region II as the lower percentage of available oxygen in the flame is offset by the slightly higher temperatures. The degree of oxidation in region III, however, increases with temperature. That is, the temperature on the substrate will increase, if no steps are taken to manage the temperature, and due to the relatively longer times that the surface is exposed to the atmosphere, the extent of interlayer oxidation is augmented.

The third and most oxidizing condition occurs when the particles or significant portions thereof are hot enough to splash or fragment upon impact. Not only will the oxidation rates of the particles be higher in regions I and II because the metal is molten, but during fragmentation, the area exposed to the atmosphere is vastly increased. The extent of oxidation in region III is compounded by the higher substrate and coating temperatures that accompany these conditions.

In Figure 4, the effect of the normalized oxygen/fuel ratio,  $\lambda$ , on the coating oxygen content for the DJ Hybrid and JP-5000

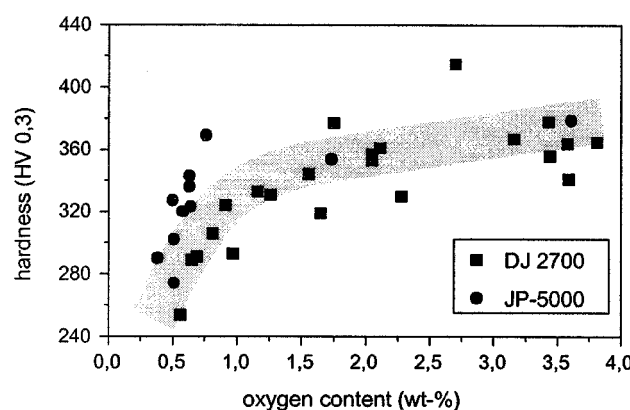


**Fig. 5** Hardness *vs* oxygen content of the coatings

systems is displayed. Where the DJ Hybrid systems apply the classical approach of spraying with a fuel-rich mixture to limit oxygen pick-up, the JP-5000 system selects overstoichiometric conditions. It is believed that the difference in the method of particle injection plays a decisive role. Powder feedstock processed with the DJ Hybrid systems is injected directly into the combustion chamber and before the throat of the de Laval nozzle. The powder thus encounters maximum flame temperatures and the oxygen content of the coatings is greatly affected by the oxygen content of the flame. In the JP-5000 system, powder is radially injected into the flame after the combustion chamber and the throat of the de Laval nozzle, where the jet temperature is about 800 K less than the maximum flame temperature, as calculated by Thorpe and Richter.<sup>[12]</sup> This and a further cooling of the flame by excess oxygen results in such low particle temperatures that oxidation rates with the oxygen in the jet and in the atmosphere become very low. In contrast, in the DJ Hybrid systems, the particles enter the jet at a considerably higher flame temperature where excess oxygen can serve to enhance the autocatalytic oxidation process.

#### 4.3 Coating Properties

Figure 5 presents a plot of microhardness versus oxygen content of all the coatings investigated. As can be observed, no clear correlation exists between hardness and oxygen content, although hardness tends to increase with oxygen content. From a

practical point of view, the hardness test can only provide a rough estimate of the oxygen level and should be used judiciously.

For the JP-5000 system, the O/F ratio most strongly influenced microhardness. As  $\lambda$  was increased from 0.82 to 1.62 at a constant pressure of 0.66 MPa, the microhardness decreased from 380 to 290 HV 0.3. Curtailing the combustion chamber pressure from 0.84 to 0.66 MPa at  $\lambda = 1.47$  reduced hardness from 370 to 290 HV 0.3. Lengthening the stand-off distance from 360 to 460 mm at reference parameters led to a decrease in microhardness from 320 to 275 HV 0.3. No significant change in microhardness was observed when spraying at higher translational velocities, to greater thicknesses, or with coarser powder. Based on these results, it is clear that mechanical deformation caused by high particle impact velocity is the dominant factor for higher hardness of coatings sprayed with the JP-5000 system. Although it could be argued that a decrease in  $\lambda$  at 0.66 MPa is not only accompanied by higher coating hardness but also higher oxygen contents, the heat treatment results confirm that no correlation exists between hardness and oxygen content within the range of 0.4 to 3.6% oxygen.

Also coatings produced with the DJ Hybrid systems reveal a trend of increasing microhardness with oxygen content. Although no clear correlations between oxygen content and hardness are apparent, results show that at values of less than 1%, the hardness for coatings generated with a propane flame is lower than 300 HV 0.3. When operating the torch with hydrogen, hardnesses less than 330 HV 0.3 signify coating oxygen contents of less than 1.2%. Alternatively, hardness greater than 350 HV 0.3 indicates that the oxygen content is greater than 2% for coatings produced by propane, hydrogen and ethylene generated flames. Lastly, an increase in gas flow is accompanied by a higher hardness for both a stoichiometric and understoichiometric flame.

The results of the bond strength tests reveal that values from 50 to 60 MPa may be realized by both spray systems when the

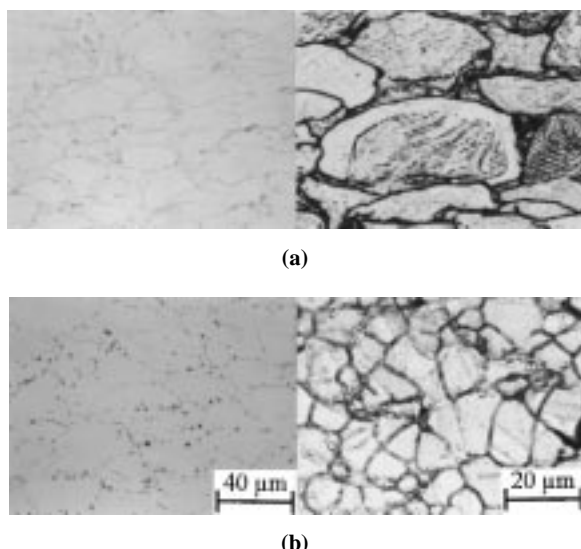


**Fig. 6** Influence of heat treatment on the coatings microstructure. (a) Before heat treatment: unmelted particles encompassed by a thin layer of oxide. (b) After heat treatment: coagulation of oxides and recrystallization to a fine-grained structure

velocity and temperature of the particles are high enough upon impact. For the JP-5000 system, this correlates to coating oxygen contents greater than 0.5%. A reduction in particle velocity and temperature by lowering the chamber pressure from 0.66 MPa to 0.59 MPa at  $\lambda = 1.18$  reduces the bond strength to 33 MPa. Similarly, increasing  $\lambda$  from 1.47 to 1.62 at a chamber pressure of 0.66 MPa decreases the bond strength to 39 MPa. Increasing the stand-off distance from 360 to 460 mm at  $\lambda = 1.36$  and a pressure of 0.66 MPa leads to a decrease in bond strength to 26 MPa. When the powder feed rate is doubled to 225 g/min, a reduction to 16 MPa is observed.

High bond strengths of 50 to 60 MPa are achieved with the DJ Hybrid systems when the coating oxygen content is greater than 0.7%. The strength, however, drops to 40 MPa when the  $\lambda$  values or the gas flow rates are considerably lower than the standard values.

Good adherent coatings with low oxygen contents may be attained, as described by Vogggenreiter *et al.*<sup>[11]</sup> when the coatings are produced under spray conditions, which lead to very low particle temperature, and then heat treated in a vacuum furnace to improve cohesion and adhesion. However, a postspray heat treatment may be impractical for most industrial applications.

#### 4.4 Influence of Heat Treatments on Coating Microstructure

The influence of heat treatment on microstructure is most readily observed in coatings with low oxygen contents. As can be seen in Fig. 6(a), the coating structure is dominated by unmelted particles encompassed by a thin layer of oxide. Etching reveals a dendritic structure within the particles. The effects of a heat treatment of 2 h at 1100°C at  $1 \times 10^{-2}$  mbar are presented in Fig. 6(b). The formerly continuous oxide layer has broken itself up by forming oxide spheres, and it is readily evident that the particle microstructure has been dissolved in favor of a classical fine-grained one. In addition, metallurgical bonding between the unmelted particles is readily observed. These two changes in microstructure alone should help prevent corrosive liquids from penetrating the coating between particles. Furthermore, etching of the substrate reveals metallurgical bonding between the substrate and the coating. Bond strength was determined to be greater than 85 MPa as the specimen broke in the glue. The hardness of the heat-treated coatings was reduced to values of between 150 and 220 HV 0.3, due to the coagulation of the oxides and the recrystallization of the deformed structure.

#### 4.5 Corrosion Results

In the Kesternich test, the coatings underwent an unusually long testing period of 25 cycles. Initial evaluations provided some startling results, namely, that coatings with low oxygen contents (<1.5%) fared worse than more oxidized coatings. In Fig. 7(a), an apparently fully dense, low oxygen coating has been detached from the substrate by underrusting and without visible damage to the coating itself. Conversely, Fig. 7(b) displays a structure, marked by oxide layers and clusters, whose coating/substrate interface is undamaged. It has been tentatively concluded that spraying the powder feedstock at low temperatures may enable the formation of voids or even holes in the coating. A corrosive liquid that either seeps into or corrodes its way

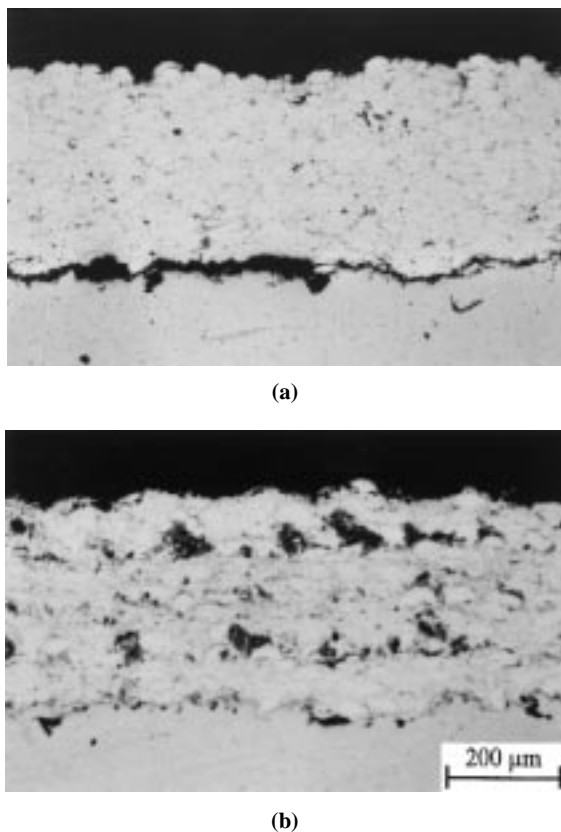


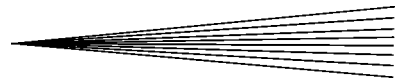
**Fig. 7** Coatings after corrosion test. (a) Underrusting of a coating with low oxide coating. (b) Good resistance of a coating with high oxide content

into such a gap will have the necessary conditions for pitting corrosion. Upon reaching the interface, the substrate and thus the bond strength will be rapidly degraded, especially if the bond is mechanical.

## 5. Conclusions

In this study, the influence of various spray parameters for the JP-5000 and DJ Hybrid systems on 316L powder was assessed and characterized. Experimental results reveal that oxygen contents of less than 1 wt.% can be fairly easily attained with the JP-5000 system, whereas tighter control of the parameters is required for the DJ Hybrid systems.

In both cases, however, the low particle temperature required for low oxygen content coatings impaired the coating's bond and cohesive strength. Heat treating the coatings after processing reduces hardness, metallurgically improves bond strength, and enables the spheroidization of the oxide layers surrounding the unmelted particles. Alternatively, bond strengths greater than 50 MPa are achieved when spraying at conditions resulting in a higher flame temperature, which is accompanied by an oxygen content of more than 0.7%. Heat treatments assisted in revealing that the microhardness of coatings containing less than 1 % oxygen is most influenced by the extent of plastic deformation due to particle velocity, resulting in a higher density of intrinsic microstructural defects and residual stress. At oxygen contents of more than 1%, hardness is essentially



constant, presumably controlled by oxide dispersion on an intrasplat and intersplat scale.

An empirical model characterizing oxidation in the thermal spray process was expanded to explain these oxidation mechanisms in the HVOF spraying of stainless steel and is used to develop parameters to minimize oxygen pickup. For these oxygen-sensitive materials, maintaining relatively low particle temperature in the spray process is critical in controlling oxygen content. For the JP-5000 system, overstoichiometric settings were used as the excess oxygen cooled the flame and the method of particle injection aided in keeping the particle temperature low. For the DJ Hybrid systems, a reduced power level and understoichiometric combustion conditions proved to be equally effective.

## Acknowledgments

The authors thank P. Heinrich and W. Krömer, Linde AG (Höllriegelskreuth, Germany), and H.-M. Höhle, Sulzer Metco Component Services GmbH (Salzgitter, Germany), for permission to conduct the spray experiments at their facilities and for their technical support.

## Conversions

1 gal = 3.785 L	1 gph = 3.785 L/h
1 ft <sup>3</sup> = 28.317 × 10 <sup>-3</sup> m <sup>3</sup>	1 scfh = 28.317 × 10 <sup>-3</sup> m <sup>3</sup> /h
1 psi = 0.06896 bar (0.6896 MPa)	

## References

1. H. Kreye, R. Schwetzkne, and S. Zimmermann: in *Thermal Spray: Practical Solutions for Engineering Problems*, C.C. Berndt, ed., ASM International, Materials Park, OH, 1996, pp. 451-56.
2. L.N. Moskowitz: in *Thermal Spray: International Advances in Coatings Technology*, C.C. Berndt, ed., ASM International, Materials Park, OH, USA, 1992, pp. 611-18.
3. C.M. Hackett and G.S. Settles: in *Thermal Spray Industrial Applications*, C.C. Berndt and S. Sampath, eds., ASM International, Materials Park, OH, USA 1994, pp. 307-12.
4. C.M. Hackett and G.S. Settles: in *Advances in Thermal Spray Science and Technology*, C.C. Berndt and S. Sampath, eds., ASM International, Materials Park, OH, 1995, pp. 21-29.
5. S. Zimmermann and H. Kreye: in *Advances in Thermal Spray Science and Technology*, C.C. Berndt and S. Sampath, ed., ASM International, Materials Park, OH, 1995, pp. 297-301.
6. S. Zimmermann: Ph.D. Thesis, Fortschritt Berichte VDI, VDI Verlag GmbH, Düsseldorf, Germany, 1997.
7. H. Kreye: Universität der Bundeswehr Hamburg, Hamburg, unpublished results, 1997.
8. A. Vardelle, P. Fauchais, and N.J. Themelis: in *Advances in Thermal Spray Science and Technology*, C.C. Berndt and S. Sampath, eds., ASM International, Materials Park, OH, 1995, pp. 175-80.
9. R.A. Neiser, M.F. Smith, and R.C. Dykhuizen: *J. Thermal Spray Technol.*, 1998, vol. 7 (4), pp. 537-45.
10. L.N. Moskowitz and D.J. Lindley: U.S. Patent No. 5,151,308, Sept. 29, 1992.
11. H.F. Voggenreiter, H. Huber, S. Beyer, and H.-J. Spies: in *Advances in Thermal Spray Science and Technology*, C.C. Berndt and S. Sampath, eds., ASM International, Materials Park, OH, 1995, pp. 303-08.
12. M.L. Thorpe and H.J. Richter: *J. Thermal Spray Technol.*, 1992, vol. 1 (2), pp. 137-47.
13. C.M. Hackett and G.S. Settles: in *Thermal Spray: Practical Solutions for Engineering Problems*, C.C. Berndt, ed., ASM International, Materials Park, OH, 1996, pp. 665-73.